

# Diminazene Ameliorates Neuroinflammation by Suppression of Astrocytic miRNA-224-5p/NLRP3 Axis in Alzheimer's Disease Model

XiaoJin Sun<sup>1,\*</sup>, Yang Deng<sup>2,\*</sup>, PengXin Ge<sup>3,\*</sup>, Qiang Peng<sup>4</sup>, Ismatullah Soufiany<sup>4</sup>, Lin Zhu<sup>4</sup>, Rui Duan<sup>4</sup>

<sup>1</sup>Faculty of Pharmacy, Bengbu Medical College, Anhui Engineering Technology Research Center of Biochemical Pharmaceuticals, Bengbu, Anhui, People's Republic of China; <sup>2</sup>School of Basic Medicine and Clinical Pharmacy, China Pharmaceutical University, Nanjing, People's Republic of China; <sup>3</sup>Department of Pharmacy, Anhui Provincial Cancer Hospital, The First Affiliated Hospital of USTC, Division of Life Sciences and Medicine, University of Science and Technology of China, Hefei, People's Republic of China; <sup>4</sup>Department of Neurology, Nanjing First Hospital, Nanjing Medical University, Nanjing, People's Republic of China

\*These authors contributed equally to this work

Correspondence: Lin Zhu; Rui Duan, Email [julinzz@163.com](mailto:julinzz@163.com); [duanruicpu@163.com](mailto:duanruicpu@163.com)

**Purpose:** ACE2/Ang(1–7)/Mas Receptor, the momentous component of the renin-angiotensin system, has been shown to be involved in Alzheimer's disease (AD). We had previously found that enhancing brain ACE2 activity ameliorated cognitive impairment and attenuated brain neuroinflammation in SAMP8 mice, an animal model of AD. However, the exact mechanism of action of Diminazene (DIZE) has not been revealed.

**Methods:** APP/PS1 mice were injected intraperitoneally with DIZE. Cognitive functions, neuronal and synaptic integrity, and inflammation-related markers were assessed by Morris water maze, Nissl staining, Western blotting and ELISA, respectively. Since astrocytes played a crucial role in AD-related neuroinflammation whilst miRNAs were reported to participate in modulating inflammatory responses, astrocytes of APP/PS1 mice were then isolated for high-throughput miRNAs sequencing to identify the most differentially expressed miRNA following DIZE treatment. Afterward, the downstream pathway of this miRNA in the anti-inflammatory action of DIZE was investigated using primary astrocytes.

**Results:** The results showed that DIZE alleviated cognitive impairment and neuronal and synaptic damage in APP/PS1 mice. Simultaneously, DIZE suppressed the secretion of pro-inflammatory cytokines and the expression of NLRP3 inflammasome. Importantly, miR-224-5p was significantly up-regulated in the astrocytes of APP/PS1 mice treated by DIZE, and NLRP3 is one of the targets of miR-224-5p. Upregulation of miR-224-5p inhibited the expression of NLRP3 in A $\beta$ 1–42-stimulated cells, whereas miR-224-5p downregulation reversed this effect. Furthermore, the inhibition of miR-224-5p could reverse the inhibitory effect of DIZE on astrocytic NLRP3 inflammasome.

**Conclusion:** These findings firstly suggested that DIZE could inhibit astrocyte-regulated neuroinflammation via miRNA-224-5p/NLRP3 pathway. Furthermore, our study reveals the underlying mechanism by which DIZE suppresses neuroinflammatory responses in AD mice and uncovers the potential of DIZE in AD treatment.

**Keywords:** DIZE, miRNA-224-5p, astrocyte, NLRP3, neuroinflammation, Alzheimer's disease

## Introduction

Alzheimer's disease (AD) is a neurodegenerative disease characterized by cognitive impairment and memory loss that lead to dementia. The main pathological hallmarks of AD are neuroinflammation, intraneuronal phosphorylated tau accumulation, and extracellular amyloid plaques.<sup>1–3</sup>

Renin-angiotensin system (RAS) is distributed in the brain, heart, colon, kidney, liver, lung and other tissues, and plays vital roles in regulating blood pressure and maintaining water and electrolyte balance. RAS in the brain is closely related to neurodegenerative diseases.<sup>4,5</sup> Recent findings show that Ang-(1-7) activation of MasR signaling or

induction of ACE2, is neuroprotective against neurogenic hypertension and ischemic stroke in the injury models of central nervous system.<sup>6,7</sup> ACE2 activity, mainly responsible for the transformation of Ang-II to Ang-(1-7)<sup>8,9</sup> was decreased by nearly 50% in AD patients, which was markedly associated with the levels of Tau and A $\beta$ .<sup>10</sup> In the ovariectomised D-galactose animal models of dementia and aging, an increase in ACE2 activity by DIZE treatment could alter brain A $\beta$  pathological features and enhance cognitive performance.<sup>11</sup> Besides, an ACE2 activator (DIZE), ameliorated A $\beta$ -associated pathological features, reversed cognitive functions in symptomatic aged Tg2576 mice, and prevented cognitive impairment in pre-symptomatic (younger) Tg2576 mice.<sup>12</sup> However, the potential mechanism is still unclarified.

Growing evidence has proven that neuroinflammation plays a vital role in this process, while astrocytes were found to be one of the predominant cells involved in neuroinflammatory responses.<sup>13,14</sup> The pro-inflammatory reactive astrocytes upregulated several complement cascade genes and induced pro-inflammatory factors, which have been reported to exert detrimental effects.<sup>11</sup> Thus, targeting astrocyte-regulated neuroinflammation may be an effective strategy in AD therapy.

MiRNAs are small non-coding RNA, normally 18–25 nucleotides, which play a key role in modulating neuroinflammatory responses.<sup>15</sup> Several studies reported that miRNAs were involved in astrocyte-regulated neuroinflammatory responses. Wang et al found miRNA-194-5p suppressed the activation of LPS induced astrocytes via neurexophilin 1.<sup>16</sup> Fang et al found that miRNA-141-3p mediated neuroinflammatory responses by inhibiting HMGB1 in *Streptococcus pneumoniae*-induced astrocytes and bacterial meningitis rat model.<sup>17</sup> Thus, APP/PS1 mice and primary astrocytes (PAs) were employed to determine whether miRNAs are responsible for the anti-inflammatory effects of DIZE on AD progression.

In view of this evidence, we then employed primary astrocytes and APP/PS1 mice to investigate whether miRNAs were involved in the anti-inflammatory action of DIZE during AD progression.

## Materials and Methods

### Animals

Male wild-type (WT) and APP/PS1 mice were supplied by Zhishan Company (Beijing, China). All animals were maintained under a 12/12-h day/night cycle, with unlimited access to drinking water and food. The ethical approval was obtained from the laboratory animal welfare and ethics. The experimental protocol was approved by the ethical committee of Nanjing First Hospital (IACUC-1911032), which was conducted in accordance with the Guide for the Care and Use of Laboratory Animals of the National Institutes of Health.

### Treatment

Mice (7 months) were intraperitoneally injected with DIZE (15 mg/kg, MedChemExpress, USA) or vehicle (0.9% sterile saline) once daily for 1 month. The route and dose of DIZE administration were selected based on a previous study.<sup>18</sup> During the whole experimental period, the general health of mice was monitored. No significant adverse reactions or obvious changes in their food intake and body weight were observed. For cell experiment, Oligomeric A $\beta$ 1-42 (Abcam, USA) was prepared as previously described, and then diluted to 5  $\mu$ M with DMEM/F12. The doses of A $\beta$ 1-42 and DIZE in cell experiment were selected according to previous studies.<sup>19,20</sup>

### Morris Water Maze (MWM)

MWM tests were conducted according to a previous study.<sup>21</sup> After drug administration, mice underwent the MWM tests. All animals were subjected to 4 trials daily for 5 days, and were given 1 min to explore the platform. After completion of each trial, all mice were placed on the platform and allowed to stay there for 30s.<sup>21</sup> The tracks of the mice were recorded using an infrared camera mounted on top of the circular pool. The EthoVision XT 10.5 software was used to record all data.

## Western Blotting (WB)

WB was conducted as described previously.<sup>22</sup> The whole brain or PAS of mice were homogenized in RIPA buffer, followed by centrifugation (12,000 g, 10 min, 4 °C). Total protein content was detected using a BCA assay kit (Thermo Fisher, MA, USA). An equivalent volume of protein (30 µg) was separated through SDS-PAGE and transferred onto a PDVF membrane. After inhibiting with 5% non-fat milk for 60 min, the membrane was exposed to primary antibodies: rabbit anti-Mas1 (1:1000; #ab235914, Abcam plc., USA), rabbit anti-synaptophysin monoclonal (1:1000; #4329, Cell Signaling Technology [CST], USA) or rabbit anti-NLRP3 (1:1000; #15101, CST) overnight at 4 °C. Anti-β actin (1:1000; #4970, CST) was employed as a loading control. The membrane was then exposed to goat anti-rabbit secondary antibodies (1:5000; #7074, CST) for 120 min. The immune complex was detected by peroxidase using an enhanced chemiluminescence system (Thermo Fisher, USA). Quantity One software (BioRad, USA) was applied to quantify the densities of protein bands.

## Nissl Staining

Nissl staining was carried out as described previously.<sup>21</sup> Following perfusion, the brain tissues were fixed for 2 days, dehydrated, embedded in paraffin wax, and then dehydrated with xylene, absolute ethanol, 95%, 80%, 70% alcohol, and distilled water. The brain sections (4 µm in thickness) were stained with Nissl staining, followed by Cresyl Violet acetate for 10 min. After rinsing with ddH<sub>2</sub>O, the sections were dehydrated with 70%, 80%, and 95% alcohol for 2 min. After washing twice with anhydrous ethanol (5 min each wash), the sections were rinsed twice with xylene (5 min each rinse). Next, the cell morphology of the hippocampus and cortex was examined by microscopy. Compared to normal neurons, the cell bodies of damaged neurons were shrunken and the nuclei stained darker. The positively stained cells were counted with ImageJ software. A total of 5 random ROIs were chosen for quantitative analysis, and the mean values were statistically calculated. The “Nissl positive neurons %” was determined by positive neurons/total neuronal cells.

## ELISA

ELISA was performed as previously described.<sup>22</sup> The whole brain was homogenized in normal saline (0.9%, for animal experiments), and the supernatant medium of PAs was collected (for cell experiment). Following centrifugation (12,000 rpm, 20 min), the supernatant was harvested and kept at -80 °C until subsequent analysis. The levels of Ang-(1-7) (abx153636; Abnova Ltd, Cambridge, UK), Aβ<sub>1-42</sub> (KMB3441, Thermo Fisher Scientific, Waltham, MA, USA), tumor necrosis factor-α (TNF-α) (ELM-TNFα-CL, Ray Biotech, Atlanta, USA), interleukin-6 (IL-6) (ab100713, abcam) and interleukin-1β (IL-1β) (#MLB00C, R&D Systems, Minnesota, USA) were determined by commercial ELISA kits. The standard curves of absorbance were used to determine the final concentrations of cytokines.

## Measurement of ACE2 Activity

The ACE2 activity assay kit containing Mc-Ala/Dnp fluorescence resonance energy transfer peptides (#AS-72086, AnaSpec, CA, USA) was employed to evaluate the activities of ACE2 in the whole brain as described previously.<sup>9</sup> The fluorescent intensities of Mc-Ala were determined at emission/excitation 390 nm/330 nm.

## qRT-PCR Assays

qRT-PCR was conducted as described previously.<sup>18</sup> The whole brain or PAs were homogenized and mixed with Trizol reagent for RNA extraction. The yields of RNA were assessed using a Nanodrop 2000 spectrophotometer. cDNA synthesis was conducted using a cDNA Synthesis Supermix (TAKARA, Japan). qRT-PCR assays were performed using the SYBR qPCR Supermix Plus (TAKARA, Japan). β-actin was used to normalize gene expression data. To detect miRNA expression, total RNA was reverse transcribed and then mixed with TaqMan Universal PCR Master Mix (TAKARA, Japan) and miRNA-specific TaqMan primers (Springen, Nanjing, China). MiRNA expression data were normalized to U6 RNA. The fold-change of gene expression was measured using the  $2^{-\Delta\Delta C_t}$  method.<sup>18</sup> All primer sequences for qRT-PCR are presented in [Supplementary Table S1](#).

## Isolation of Adult Astrocytes

Isolation of adult astrocytes was performed as described previously.<sup>22</sup> Magnetic isolation of the astrocytes from adult WT and APP/PS1 mouse brain tissues, was conducted using the Adult Brain Dissociation Kit and ACSA-2 (astrocyte) MicroBeads (Miltenyi Biotec, Germany). Briefly, the brain tissues were digested with Adult Brain Dissociation Kit and single-cell suspension was prepared. Next, debris and erythrocytes were removed. After incubation with ACSA-2 (astrocyte) MicroBeads for 15 min at 4 °C, the astrocytes were separated from single-cell suspension using the MS columns, QuadroMACS and MACS MultiStand (Miltenyi Biotec, Germany) in a magnetic field.

## miRNA Sequencing

Total RNA was extracted using a Trizol kit (Takara, Japan). The integrity and yield of RNA were evaluated by Agilent 2100 Bioanalyzer (Agilent, CA, USA) and Nanodrop (Bio-Rad, CA, USA), respectively. RNA samples were first ligated with a 3' adapter, and then fragmented into smaller sizes and ligated to 5' adapter. Next, the small RNA library was constructed and sequenced by Gene Denovo Biotechnology (Guangzhou, China) using the Illumina Novaseq 6000 platform. After the sequence reads were trimmed and filtered, subsequent RNA-seq reads were mapped to GenBank, Rfam, Genome and miRBase databases. Differential miRNA expression was evaluated using the EdgeR software. All sequencing data were deposited in GenBank (GSE199028).

## Culture of PAs

Culture of PAs was conducted as previously described.<sup>22</sup> Briefly, the whole brain of C57Bl/6 mice was chopped at postnatal day 1. A 70- $\mu$ m nylon mesh was used for mechanical mincing. The glial cells were cultured in DMEM/F12 containing FBS (10%), streptomycin (100  $\mu$ g/mL), and penicillin (100 unit/mL) at 37 °C and 5% CO<sub>2</sub> for 14 days. To isolate PAs, the 75 T flask was sealed with foils and shaken at 250 rpm overnight. After discarding the conditioned culture medium, trypsin-ETDA was used to dissociate the cells. After centrifugation (2000 rpm, 30 min), the PAs were harvested for subsequent analyses.

## Transient Transfection

Transient transfection was conducted as described previously.<sup>23</sup> Briefly,  $2 \times 10^5$ /mL PAs were seeded in a 6-well plate. Upon reaching 70% confluence, the transient transfection of miRNA mimics or inhibitors was conducted with lipofectamine 2000 (Invitrogen, CA, USA). The transfection reagent complexes with miRNA mimics or inhibitors (100 nM) were added to each well. After incubation for 6 h at 37 °C, the cell medium was replaced with 10% FBS-containing DMEM/F12. The miRNA mimic and inhibitor sequences are presented in [Supplementary Table S2](#).

## Dual-Luciferase Reporter (DLR) Assays

Targetscan 7.2 ([http://www.targetscan.org/vert\\_72/](http://www.targetscan.org/vert_72/)) was used to identify the possible miRNAs bound to the 3'-UTR sequences of NLRP3, and predict the binding site between miRNA-224-5p and NLRP3. The baseline data and species conservatism of miRNA-224-5p were retrieved from the UCSC database (<http://genome.ucsc.edu/>). The 293T cells were cotransfected with Mut and WT NLRP3 3'-UTR reporter constructs in the presence of miRNA-224-5p mimics or NC mimics via lipofectamine 2000. Following transfection for 2 days, the cells were harvested and evaluated by a DLR assay system (Promega, WI, USA).

## CCK8 Assays

Cell viability was assessed by Cell Counting Kit-8 (CCK8; Beyotime, Shanghai, China) assays. The astrocytes ( $1 \times 10^4$  cells/well) were grown in a 96-well plate for 1 day at 37°C. Subsequently, the cells were treated with different concentrations (0, 0.001, 0.01, 0.1, 1 mM) of DIZE. After treatment for 2 days, CCK-8 reagent (10  $\mu$ L) was added, and maintained for 2 h. All assays were conducted in triplicate. The absorbance was detected using a microplate reader (Bio-Rad) at 450 nm. The wells without cells were used as blanks. Cell viability was calculated based on the absorbance.

## Statistical Analysis

All values are shown as mean  $\pm$  standard deviation (SD). Statistical tests were conducted with GraphPad Prism 8. Student's *t*-test was applied for comparing the difference between two groups, whereas one-way ANOVA followed by Tukey's post-hoc test was applied for comparing the differences among multiple groups. MWM was analyzed with two-way repeated-measures ANOVA and then Bonferroni's multiple comparisons test.  $P < 0.05$  was deemed statistically significant.

## Results

### ACE2/Ang-(1-7)/MAS1 Pathways are Activated by DIZE in the Brain Tissues of APP/PS1 Mice

As displayed in [Figure 1A](#), the brain levels of Ang-(1-7) were dramatically lower in APP/PS1 mice than in WT controls. Treatment with 15 mg/kg DIZE remarkably elevated the brain activity of Ang-(1-7) and ACE2 in APP/PS1 mice ([Figure 1A](#) and [B](#)). The mRNA levels of Mas1 were upregulated in the brain tissues of APP/PS1 mice after DIZE administration ([Figure 1C](#)), and its protein level also exhibited a similar increasing trend ([Figure 1D](#) and [E](#)).

### DIZE Ameliorates Cognitive Deficits and Exhibits Neuroprotective Effects Against AD

MWM test was performed 5 days before sacrificing the mice. As revealed in [Figure 2A](#), APP/PS1 mice had obviously worse performance compared with their age-matched controls, suggesting that spatial cognitive impairment is observed in AD mice. Treatment with DIZE ameliorated spatial cognitive impairment in APP/PS1 mice ([Figure 2A](#)). Meanwhile, as shown in [Figure 2B](#), no difference in swimming speed was found between WT controls and APP/PS1 mice. Treatment with DIZE did not affect swimming speed in APP/PS1 mice ([Figure 2B](#)) and control mice. As demonstrated in [Figure 2C](#) and [D](#), APP/PS1 mice had obvious synaptic loss (as revealed by the protein levels of synaptophysin) compared to control mice. Furthermore, a significant neuronal loss (as revealed by positive Nissl staining) in the cortex was also detected in the brain tissues of APP/PS1 mice ([Figure 2E](#) and [F](#)). However, DIZE administration had no effect on the proportion of Nissl-positive neurons in the hippocampus ([Supplementary Figure 1](#)). As displayed in [Figure 2C](#) and [D](#), DIZE administration increased the protein levels of synaptophysin as well as the proportion of Nissl-positive neurons in the cortex ([Figure 2E](#) and [F](#)).

### DIZE Attenuates Neuroinflammatory Responses in APP/PS1 Mice

As demonstrated in [Figure 3A–C](#), the mRNA levels of TNF- $\alpha$ , IL-6 and IL-1 $\beta$  were markedly higher in APP/PS1 mice than in control mice. Treatment with DIZE remarkably decreased the transcriptional levels of these pro-inflammatory cytokines in APP/PS1 mice ([Figure 3A–C](#)). As demonstrated in [Figure 3D–F](#), the protein levels of TNF- $\alpha$ , IL-6 and IL-1 $\beta$  were markedly higher in APP/PS1 mice than in control mice. Treatment with DIZE remarkably decreased the protein levels of these pro-inflammatory cytokines in APP/PS1 mice ([Figure 3D–F](#)).

### DIZE Reduces the Level of A $\beta_{1-42}$ in APP/PS1 Mice

As displayed in [Figure 4](#), The level of A $\beta_{1-42}$  was dramatically higher in APP/PS1 mice than in WT controls. Treatment with DIZE remarkably reduced A $\beta_{1-42}$  level in the brain of APP/PS1 mice ([Figure 4](#)).

### miRNA-224-5p Participates in the Inhibitory Effect of DIZE on NLRP3 Inflammasome in Astrocytes

Astrocytes play a crucial role in AD-related neuroinflammation accompanied by marked activation of the NLRP3 inflammasome.<sup>24</sup> To assess whether DIZE can exert an inhibitory effect on astrocytic NLRP3 inflammasome, the PAs were isolated from AD mice with/without DIZE injection. As demonstrated in [Figure 5A](#) and [B](#), the PAs from AD mice without DIZE administration had a dramatically higher protein level of NLRP3 than those from control mice, suggesting that NLRP3 inflammasome is activated in the astrocytes of AD mice. The PAs from DIZE-treated APP/PS1 mice showed a remarkable decrease in the protein expression of NLRP3 ([Figure 5A](#) and [B](#)), suggesting that NLRP3 inflammasome is suppressed in astrocytes after DIZE treatment.

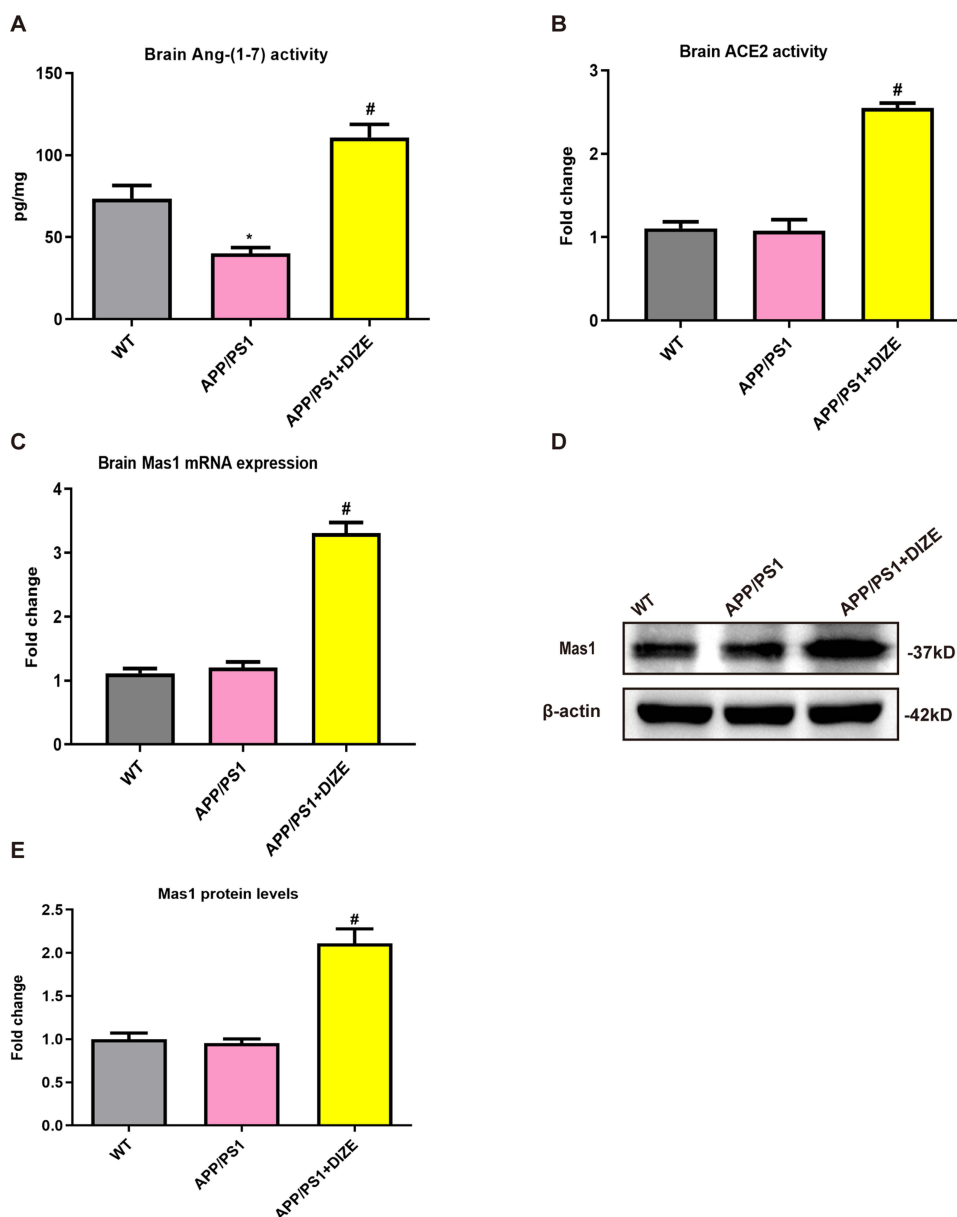


**Figure 1** DIZE activates ACE2/Ang-(1-7)/MAS1 axis in the brain of APP/PS1 mice. **(A)** The levels of Ang-(1-7) in mouse brain tissues were detected by ELISA ( $n = 6$  per group). **(B)** The activity of ACE2 in mouse brain tissues was assessed using a commercial ACE2 activity assay kit ( $n = 6$  per group). **(C)** The mRNA levels of Mas1 in mouse brain tissues were evaluated by qRT-PCR, and  $\beta$ -actin was used as an internal control ( $n = 6$  per group). **(D)** The protein levels of MAS1 in mice brain were detected by Western blotting.  $\beta$ -actin was used as a loading control ( $n = 6$  per group). **(E)** Quantitative analysis of MAS1 protein levels ( $n = 6$  per group). All data are expressed as means  $\pm$  SD. \* $P < 0.05$  versus age-matched vehicle-treated WT control mice. # $P < 0.05$  versus vehicle-treated APP/PS1 mice.

MiRNAs have been shown to be involved in the regulation of neuroinflammatory responses after AD.<sup>25</sup> To determine whether miRNAs are responsible for the inhibitory effects of DIZE on NLRP3 inflammasome in astrocytes, high-throughput miRNA sequencing was performed in PAs from APP/PS1 mice with/without DIZE administration. As shown in Figure 5C, 4 differentially expressed miRNAs were screened based on a threshold of  $|\log_2FC| > 1$  and corrected  $P < 0.0001$ . Meanwhile, volcano plot analysis also revealed 4 differentially expressed miRNAs in the PAs of DIZE-treated APP/PS1 mice (Figure 5D). Among them, 1 miRNA was markedly downregulated whilst the other miRNAs were remarkably upregulated. qRT-PCR data showed that miRNA-224-5p was highly expressed in the PAs of DIZE-treated APP/PS1 mice (Figure 5E).

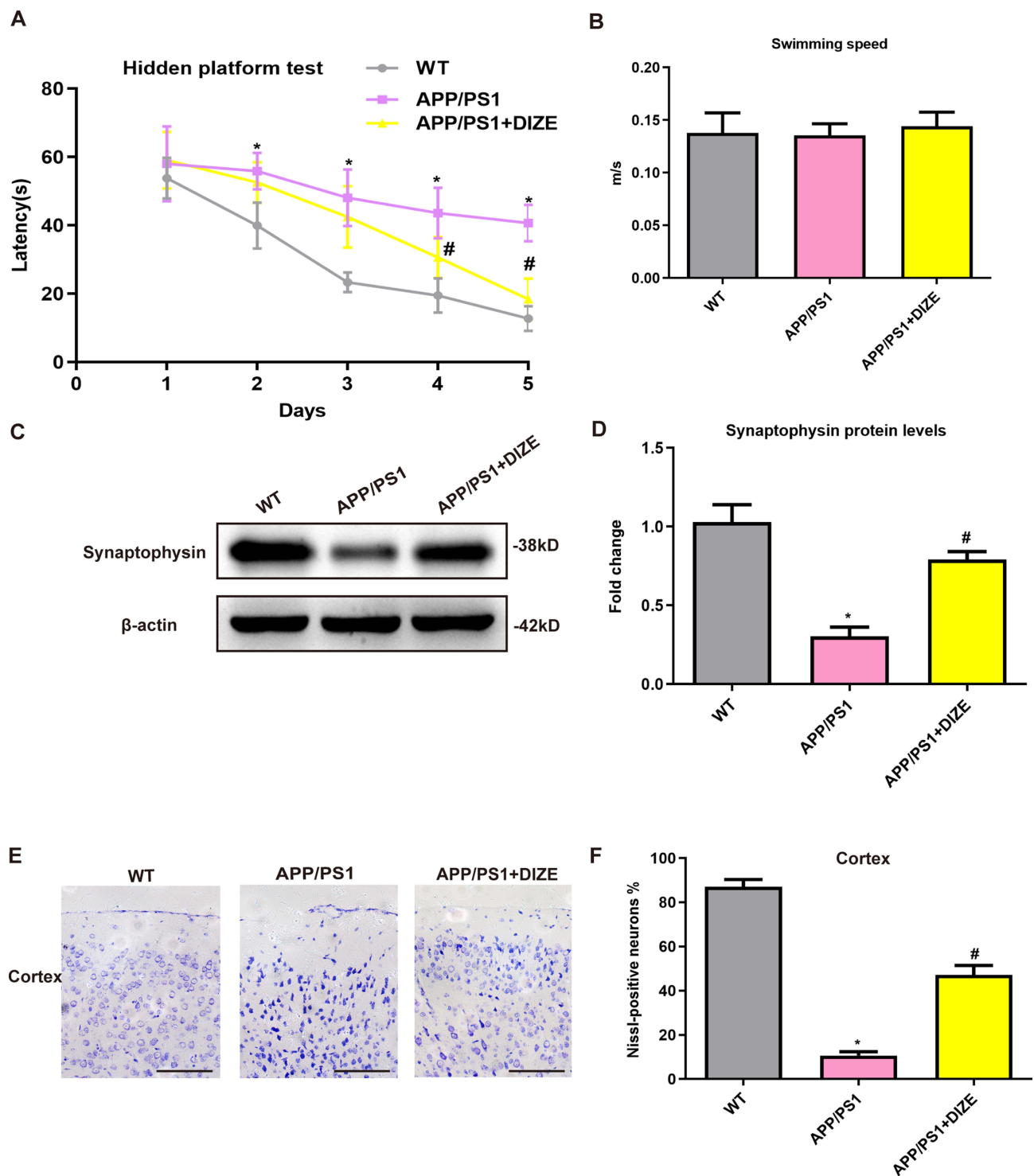


**Figure 2** DIZE rescues cognitive impairments and offers neuroprotection in APP/PS1 mice. **(A)** Path length of each group in the hidden platform test ( $n = 15$  per group). **(B)** Swimming speed of each group in the Morris water-maze test ( $n = 15$  per group). **(C and D)** Representative Western blot bands and densitometric analysis of synaptophysin in the brain.  $\beta$ -actin was used as an internal control ( $n = 6$  per group). **(E)** Neuronal loss in the cortex of mice was detected by Nissl staining. Neurons with dark violet nucleus and intact morphology were identified as Nissl-positive neurons. Scale bar =  $100 \mu\text{m}$  ( $n = 6$  per group). **(F)** Quantitative analysis of Nissl-positive neurons in the brain ( $n = 6$  per group). All data are expressed as means  $\pm$  SD. \* $P < 0.05$  versus the WT group. # $P < 0.05$  versus the APP/PS1 group.

## NLRP3 is Directly Targeted by miRNA-224-5p

Next, to determine the relationships between miRNA-224-5p and NLRP3, we first conducted miRNA prediction with Targetscan online software and DLR assays in HEK 293T cells to verify that NLRP3 was directly targeted by miRNA-224-5p. As shown in

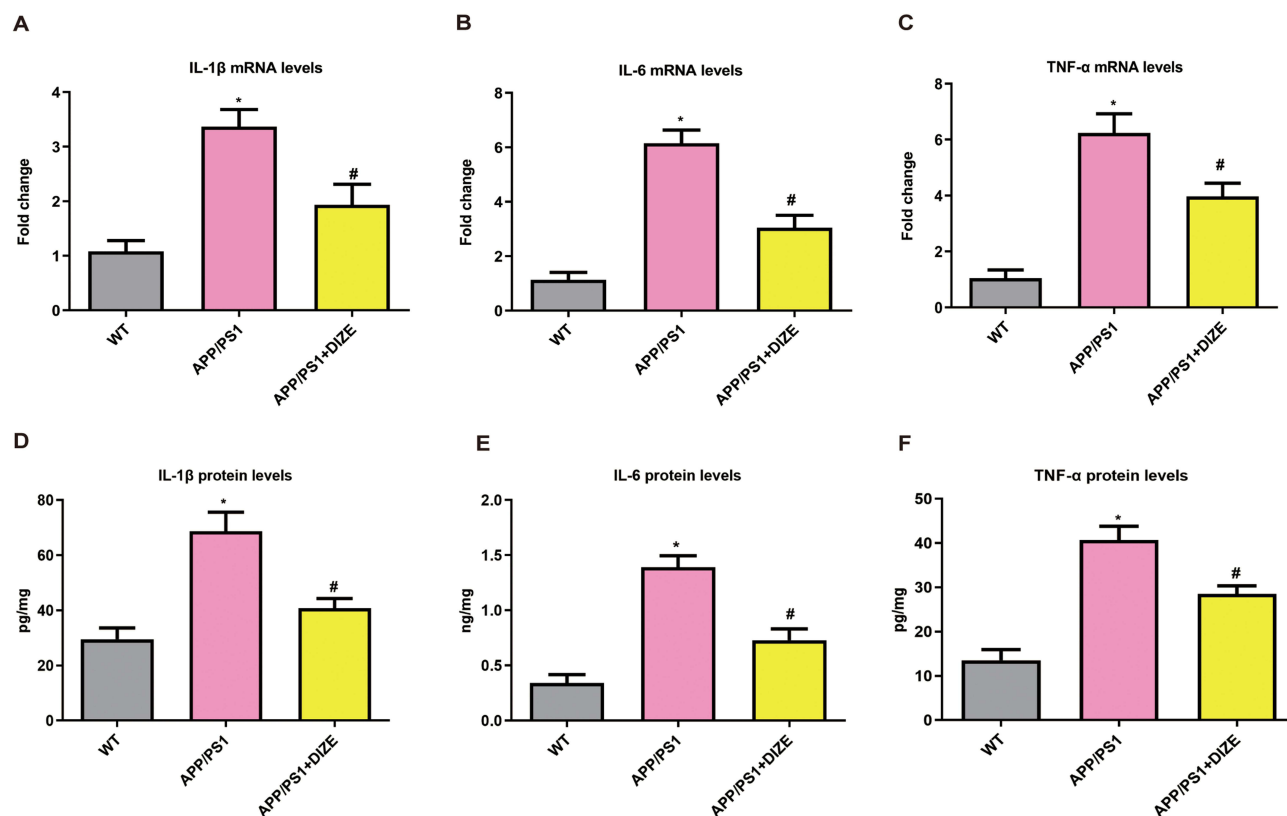


**Figure 3** DIZE suppresses neuroinflammation in APP/PS1 mice. (A–C) RT-PCR assays of IL-1 $\beta$ , IL-6 and TNF- $\alpha$  mRNA in the brain (n = 6 per group). All data are expressed as means  $\pm$  SD. \* $P < 0.05$  versus the WT group. \* $P < 0.05$  versus the APP/PS1 group. # $P < 0.05$  versus the APP/PS1 group. (D–F) ELISA assays of IL-1 $\beta$ , IL-6 and TNF- $\alpha$  protein in the brain (n = 6 per group). All data are expressed as means  $\pm$  SD. \* $P < 0.05$  versus the WT group. # $P < 0.05$  versus the APP/PS1 group.

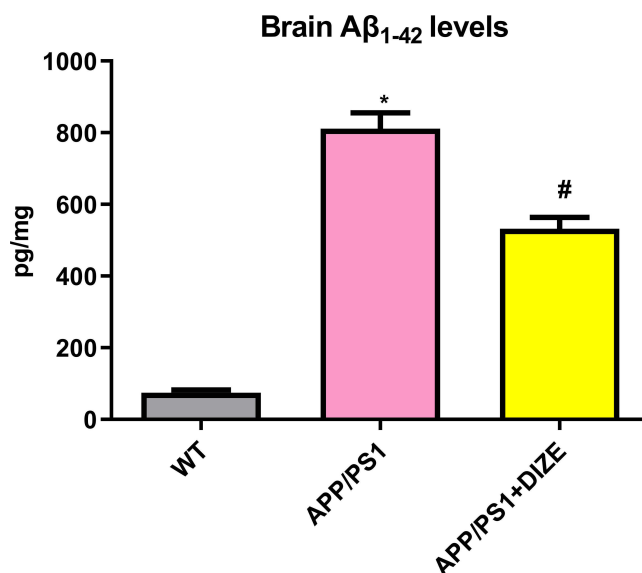


**Figure 4** DIZE rescues the level of A $\beta_{1-42}$  in APP/PS1 mice. ELISA assays of A $\beta_{1-42}$  in the brain (n = 6 per group). All data are expressed as means  $\pm$  SD. \* $P < 0.05$  versus the WT group. # $P < 0.05$  versus the APP/PS1 group.

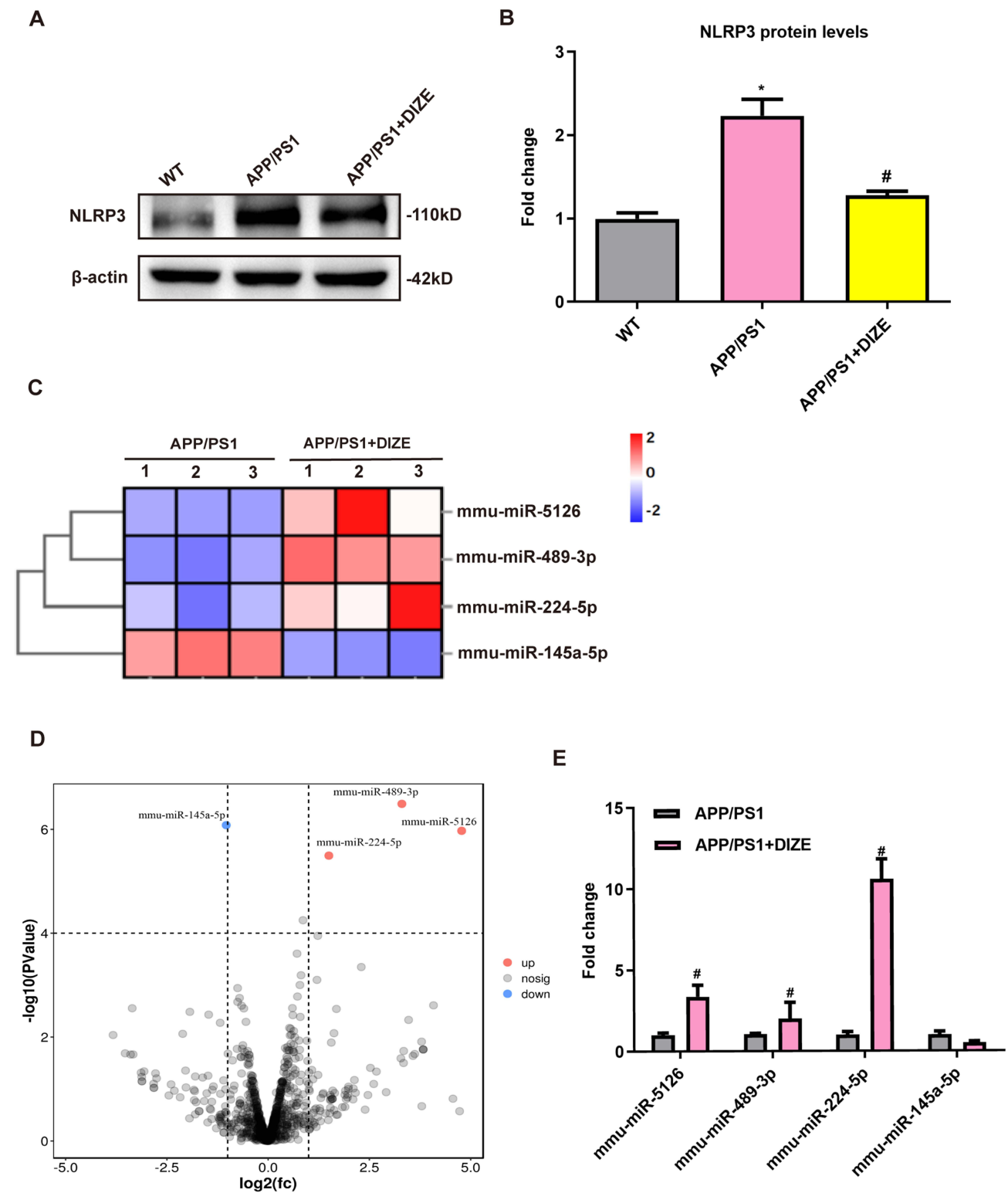


**Figure 5** miRNA-224-5p may be involved in DIZE-induced inhibition of astrocytic NLRP3 inflammasome. **(A and B)** Representative Western blot bands and densitometric analysis of NLRP3 in the brain ( $n = 6$  per group).  $\beta$ -actin was used as an internal control. **(C)** The heatmap represents hierarchical clustering for differentially expressed miRNAs in the astrocytes from adult mice ( $n = 3$  per group). **(D)** The volcano plot of DEGs. The red dots represent upregulated genes, and the blue dots represent downregulated genes ( $n = 3$  per group). **(E)** The qRT-PCR results of miRNA-5126, miRNA-489-3p, miRNA-224-5p and miRNA-145a-5p expression in the PAs from adult mice ( $n = 3$  per group). All data are expressed as means  $\pm$  SD. \* $P < 0.05$  versus the WT group. # $P < 0.05$  versus the APP/PS1 group.

Figure 6A and B, miRNA-224-5p was shown to possess binding sites with NLRP3, and it could suppress the luciferase activity of NLRP3-3'-UTR-WT, without affecting NLRP3-3'-UTR-Mut. To examine the effects of DIZE on the cytotoxicity of astrocytes, the cells were exposed to varying concentrations of DIZE for 2 days, and the cell cytotoxicity was subsequently evaluated by CCK8 assays. As demonstrated in Figure 6C, no obvious difference in cell cytotoxicity was found between the cells exposed to DIZE below 0.1 mM and control cells, but DIZE at the concentration of 1 mM significantly increased the cell cytotoxicity of astrocytes. Therefore, the DIZE concentration of 0.1 mM was chosen for subsequent analyses. As displayed in Figure 6D, A $\beta$ 1-42 markedly decreased the expression of miRNA-224-5p, and this downregulation pattern was reversed by DIZE. Moreover, miRNA-224-5p inhibitors upregulated the protein expression of NLRP3 (Figure 6E and F), whereas miRNA-224-5p mimics decreased this effect (Figure 6G and H). Furthermore, miRNA-224-5p inhibitors increased the protein expression of IL-1 $\beta$  (Figure 6I), whereas miRNA-224-5p mimics decreased this effect (Figure 6J).

## miRNA-224-5p Participates in the Inhibitory Effect of DIZE on NLRP3 Inflammasome in Astrocytes

To explore whether miRNA-224-5p can participate in DIZE-induced suppression of astrocytic NLRP3 inflammasome, the astrocytes were exposed to DIZE with/without miRNA-224-5p inhibitors. As displayed in Figure 7A and B, miRNA-224-5p inhibitors remarkably reversed DIZE-induced downregulated protein levels of NLRP3 (Figure 7A and B). Additionally, the reduced protein levels of IL-1 $\beta$  caused by DIZE were also abolished by miRNA-224-5p inhibitors (Figure 7C).

## Discussion

In this study, we found that DIZE treatment significantly improved AD-related spatial cognition impairment and suppressed neuroinflammation in APP/PS1 mice. Further high-throughput sequencing indicated that miRNA-224-5p expression was drastically upregulated in astrocytes of APP/PS1 mice after DIZE treatment, and mediated the inflammatory response through NLRP3 inflammasome. Thus, this is the first study to show that DIZE mediated astrocyte-regulated neuroinflammatory responses via miRNA-224-5p/NLRP3 pathway.

Several studies have shown that RAS is a potential contributor to dementia and ACE2/Ang-(1-7)/MAS1 axis has been demonstrated to be important.<sup>18,22,26</sup> It has been proven that in the injury models of central nervous system, inducing ACE2 or Ang-(1-7) activation of MasR signal has neuroprotective effects on neurogenic hypertension and ischemic stroke.<sup>6,7</sup> Our results indicated that the activity of Ang-(1-7), a critical regulator of ACE2/Ang-(1-7)/MAS1 pathways, was decreased in the brain tissues of APP/PS1 mice, while DIZE remarkably increased the brain levels of Ang-(1-7) and MAS1. This result is consistent with our prior finding on experimental AD models.<sup>18</sup>

Increasing evidence indicates that neuroinflammation is one of the important factors that trigger and promote AD.<sup>27–29</sup> In this study, the decreased levels of several pro-inflammatory factors imply that the neuroprotective effects of DIZE are closely related to the suppression of inflammation. It has been known that NLRP3 inflammasome can be rapidly activated after inflammation. NLRP3 inflammasome is composed of Pro-caspase-1, apoptosis-associated speck-like protein (ASC), and NLRP3. NLRP3 recognizes pathogens or endogenous danger signals, recruits and activates Caspase-1, splashes IL-18 and IL-1 $\beta$  precursors, and produces the corresponding mature cytokines that are widely involved in adaptive immune responses.<sup>30</sup> Zhang et al indicated that NLRP3 could enhance the role of NLRP3 inflammasome by increasing IL-1 $\beta$  expression through activation of NF- $\kappa$ B signaling pathway.<sup>31</sup> Our study has shown that the levels of NLRP3 were remarkably lower in the PAs from DIZE-treated AD mice than those from untreated AD mice, suggesting that NLRP3 inflammasome can be suppressed by DIZE.

MiRNAs are small non-coding RNA containing 18–25 nucleotides, which bind to the 3'-UTR region in a target gene for regulating gene expression, thus inducing degradation or inhibiting translation of the target mRNA.<sup>32,33</sup> Alterations in ncRNAs can be detected in CSF and the circulation as well as the brain, and are showing promise as biomarkers, with the ultimate goal clinical exploitation as targets for novel modes of symptomatic and course-altering therapy.<sup>34,35</sup> Several studies have reported that miRNA is abnormally expressed in the brain, plasma and cerebrospinal fluids of AD cases.<sup>36–38</sup> Several abnormally expressed miRNAs are key transcriptional activators of selected mediators of inflammation.<sup>39</sup> Based on these evidences, we hypothesize that miRNAs can participate in the regulation of DIZE-induced attenuation of NLRP3

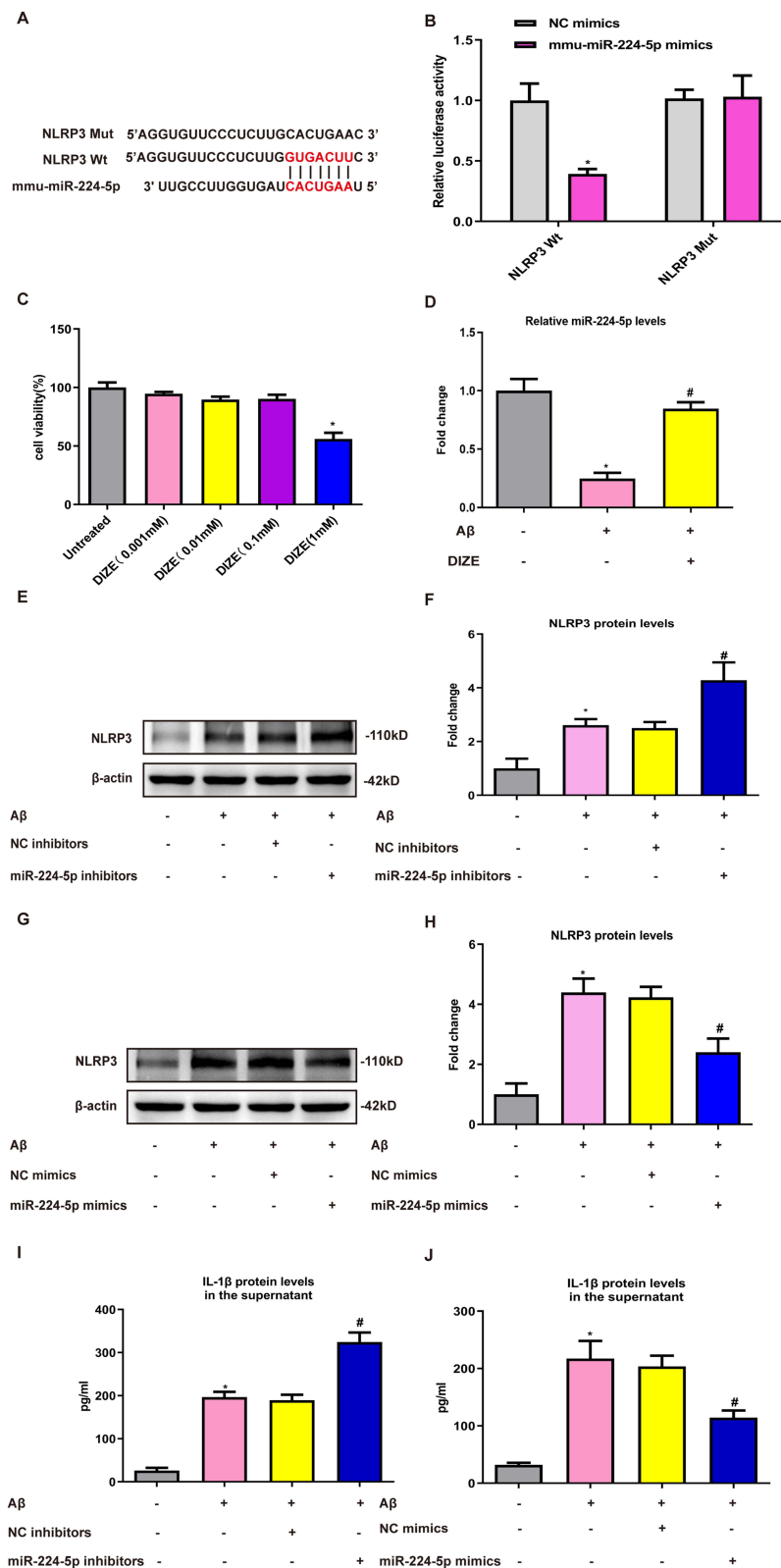


**Figure 6** NLRP3 is a direct target of miRNA-224-5p. (**A** and **B**) Luciferase reporter assay in HEK 293T cells transfected with psiCHECK2-NLRP3 (WT or Mut) and miRNA-224-5p mimics or NC mimics ( $n = 3$  per group). (**C**) The cell cytotoxicity of astrocytes treated with different concentrations of DIZE was measured by CCK-8 assay ( $n = 3$  per group). (**D**) The qRT-PCR result of miRNA-224-5p expression in the PAs following A $\beta_{1-42}$  stimulation ( $n = 3$  per group). (**E–H**) Representative Western blot bands and densitometric analysis of NLRP3 in the PAs.  $\beta$ -Actin was used as an internal control ( $n = 3$  per group). (**I–J**) ELISA assay of IL-1 $\beta$  protein in the supernatant of PAs ( $n = 3$  per group). All data are expressed as the means  $\pm$  SD of three independent experiments. \* $P < 0.05$  versus the NC mimics, untreated or NC inhibitors group. # $P < 0.05$  versus the A $\beta$ , A $\beta$ +NC inhibitors and A $\beta$ +NC mimics group.

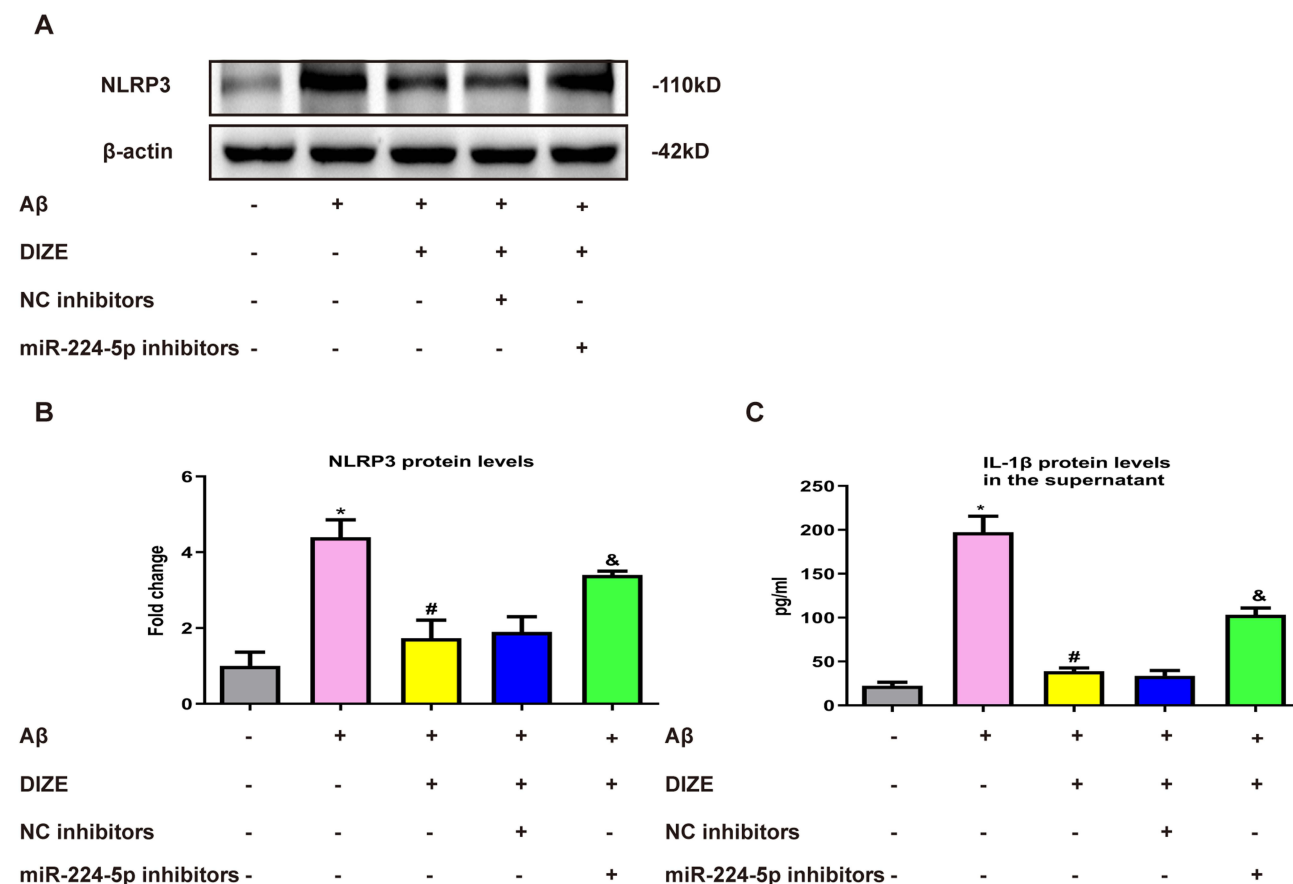


**Figure 7** miRNA-224-5p participates in the DIZE-induced suppression of astrocytic NLRP3 inflammasome. **(A and B)** Representative Western blot bands and densitometric analysis of NLRP3 in the PAs.  $\beta$ -Actin was used as an internal control ( $n = 3$  per group). **(C)** ELISA assay of IL-1 $\beta$  protein in the supernatant of PAs ( $n = 3$  per group). All data are expressed as the means  $\pm$  SD of three independent experiments. \* $P < 0.05$  versus the untreated group. # $P < 0.05$  versus the A $\beta$  group. & $P < 0.05$  versus the A $\beta$ +DIZE +NC inhibitor group.

inflammasome in astrocytes. The miRNA sequencing and qRT-PCR verification data showed that miRNA-224-5p was the most upregulated miRNA in the astrocytes of APP/PS1 mice following DIZE treatment. The results of online bioinformatics database analysis indicated that miRNA-224-5p could target NLRP3. The interactions between miRNA-224-5p and NLRP3 were verified by DLR assays, whereas the expression of NLRP3 was negatively modulated by miRNA-224-5p, suggesting that NLRP3 can be targeted by miRNA-224-5p. This result is in agreement with the finding of Du et al.<sup>40</sup> Similarly, A $\beta$  significantly downregulated the expression of miRNA-224-5p in astrocytes in vitro. However, this decrease was remarkably reversed by DIZE. Next, Western blot analysis revealed that miRNA-224-5p inhibitors increased the expression of NLRP3, while the miRNA-224-5p mimics had an opposite effect. Moreover, it was observed that miRNA-224-5p inhibitors increased the level of IL-1 $\beta$ , while miRNA-224-5p mimics had an opposite effect. Furthermore, our results also demonstrated that miRNA-224-3p inhibitors could reverse DIZE-induced attenuation of NLRP3 inflammasome, indicating that this miRNA can regulate the inhibitory effect of DIZE on NLRP3 inflammasome in astrocytes.

This study had some limitations. First, this work lacks the evidence of how DIZE upregulated the expression of miRNA-224-5p. Second, since microglia is a major cell type mediating inflammation in vivo, whether the therapeutic effect of DIZE in the APP/PS1 mice via suppression of microglia activation is not mentioned. In the future, we will analyze microglia isolated from adult APP/PS1 transgenic mice to validate our findings.

## Conclusion

In conclusion, our results demonstrated that DIZE could inhibit astrocyte-regulated neuroinflammatory responses via miRNA-224-5p/NLRP3 pathway and confer neuroprotective effects on AD (Figure 8).

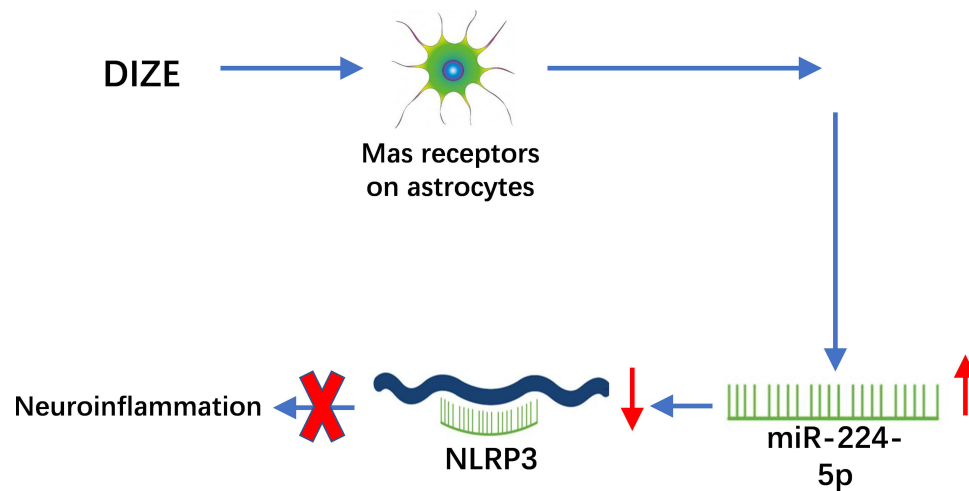


**Figure 8** A schematic figure showing DIZE inhibited astrocyte-regulated neuroinflammatory responses via miRNA-224-5p/NLRP3 pathway and provided neuroprotective effects on AD.

## Funding

This work was supported by the Natural Science Foundation of Jiangsu Province (BK20220196), Nanjing International Joint research and development Project (202201030), Project funded by China Postdoctoral Science Foundation (2022M711666), University Natural Science Project of Anhui Province (2022AH051534) and Xinghuo Talent Program of Nanjing First Hospital.

## Disclosure

The authors declare that there is no conflict of interest.

## References

1. Raskin J, Cummings J, Hardy J, Schuh K, Dean RA. Neurobiology of Alzheimer's disease: integrated molecular, physiological, anatomical, biomarker, and cognitive dimensions. *Curr Alzheimer Res*. 2015;12(8):712–722. doi:10.2174/1567205012666150701103107
2. Deardorff WJ, Grossberg GT. Targeting neuroinflammation in Alzheimer's disease: evidence for NSAIDs and novel therapeutics. *Expert Rev Neurother*. 2017;17(1):17–32. doi:10.1080/14737175.2016.1200972
3. Cai M, Lee JH, Yang EJ. Electroacupuncture attenuates cognition impairment via anti-neuroinflammation in an Alzheimer's disease animal model. *J Neuroinflammation*. 2019;16(1):264. doi:10.1186/s12974-019-1665-3
4. Royea J, Martinot P, Hamel E. Memory and cerebrovascular deficits recovered following angiotensin IV intervention in a mouse model of Alzheimer's disease. *Neurobiol Dis*. 2020;134:104644. doi:10.1016/j.nbd.2019.104644
5. Jackson L, Eldahshan W, Fagan SC, Ergul A. Within the brain: the renin angiotensin system. *Int J Mol Sci*. 2018;19(3):876. doi:10.3390/ijms19030876
6. Feng Y, Xia H, Santos RA, Speth R, Lazartigues E. Angiotensin-converting enzyme 2: a new target for neurogenic hypertension. *Exp Physiol*. 2010;95(5):601–606. doi:10.1113/expphysiol.2009.047407
7. Jiang T, Gao L, Lu J, Zhang YD. ACE2-Ang-(1-7)-mas axis in brain: a potential target for prevention and treatment of ischemic stroke. *Curr Neuropharmacol*. 2013;11(2):209–217. doi:10.2174/1570159X11311020007
8. Vickers C, Hales P, Kaushik V, et al. Hydrolysis of biological peptides by human angiotensin-converting enzyme-related carboxypeptidase. *J Biol Chem*. 2002;277(17):14838–14843. doi:10.1074/jbc.M200581200
9. Kehoe PG, Wong S, Al Mulhim N, Palmer LE, Miners JS. Angiotensin-converting enzyme 2 is reduced in Alzheimer's disease in association with increasing amyloid- $\beta$  and tau pathology. *Alzheimers Res Ther*. 2016;8(1):50. doi:10.1186/s13195-016-0217-7
10. Kamel AS, Abdelkader NF, Abd El-Rahman SS, Emara M, Zaki HF, Khattab MM. Stimulation of ACE2/ANG(1-7)/mas axis by diminazene ameliorates Alzheimer's disease in the D-galactose-ovariectomized rat model: role of PI3K/Akt pathway. *Mol Neurobiol*. 2018;55(10):8188–8202. doi:10.1007/s12035-018-0966-3
11. Liddelow SA, Barres BA. Reactive astrocytes: production, function, and therapeutic potential. *Immunity*. 2017;46(6):957–967. doi:10.1016/j.immuni.2017.06.006
12. Evans CE, Miners JS, Piva G, et al. ACE2 activation protects against cognitive decline and reduces amyloid pathology in the Tg2576 mouse model of Alzheimer's disease. *Acta Neuropathol*. 2020;139(3):485–502. doi:10.1007/s00401-019-02098-6
13. Bradburn S, Murgatroyd C, Ray N. Neuroinflammation in mild cognitive impairment and Alzheimer's disease: a meta-analysis. *Ageing Res Rev*. 2019;50:1–8. doi:10.1016/j.arr.2019.01.002
14. Morales I, Jiménez JM, Mancilla M, Maccioni RB. Tau oligomers and fibrils induce activation of microglial cells. *J Alzheimers Dis*. 2013;37(4):849–856. doi:10.1023/JAD-131843

15. Takousis P, Sadlon A, Schulz J, et al. Differential expression of microRNAs in Alzheimer's disease brain, blood, and cerebrospinal fluid. *Alzheimers Dement*. 2019;15(11):1468–1477. doi:10.1016/j.jalz.2019.06.4952
16. Wang M, Li Z, Zuo Q. miR-194-5p inhibits LPS-induced astrocytes activation by directly targeting neurexophilin 1. *Mol Cell Biochem*. 2020;471(1–2):203–213. doi:10.1007/s11010-020-03780-0
17. Fang X, Wang H, Zhuo Z, et al. miR-141-3p inhibits the activation of astrocytes and the release of inflammatory cytokines in bacterial meningitis through down-regulating HMGB1. *Brain Res*. 2021;1770:147611. doi:10.1016/j.brainres.2021.147611
18. Duan R, Xue X, Zhang QQ, et al. ACE2 activator diminazene aceturate ameliorates Alzheimer's disease-like neuropathology and rescues cognitive impairment in SAMP8 mice. *Aging*. 2020;12(14):14819–14829. doi:10.18632/aging.103544
19. Li S, Li Y, Xu H, et al. ACE2 attenuates epithelial-mesenchymal transition in MLE-12 cells induced by silica. *Drug Des Devel Ther*. 2020;14:1547–1559. doi:10.2147/DDDT.S252351
20. Yao Y, Huang JZ, Chen Y, Hu HJ, Tang X, Li X. Effects and mechanism of amyloid  $\beta$ 1-42 on mitochondria in astrocytes. *Mol Med Rep*. 2018;17(5):6997–7004. doi:10.3892/mmr.2018.8761
21. Sun X, Deng Y, Fu X, Wang S, Duan R, Zhang Y. AngIV-analog dihexa rescues cognitive impairment and recovers memory in the APP/PS1 mouse via the PI3K/AKT signaling pathway. *Brain Sci*. 2021;11(11):1487. doi:10.3390/brainsci11111487
22. Duan R, Wang SY, Wei B, et al. Angiotensin-(1-7) analogue AVE0991 modulates astrocyte-mediated neuroinflammation via lncRNA SNHG14/miR-223-3p/NLRP3 pathway and offers neuroprotection in a transgenic mouse model of Alzheimer's disease. *J Inflamm Res*. 2021;14:7007–7019. doi:10.2147/JIR.S343575
23. Yang CC, Lin CC, Hsiao LD, Kuo JM, Tseng HC, Yang CM. Lipopolysaccharide-induced matrix metalloproteinase-9 expression associated with cell migration in rat brain astrocytes. *Int J Mol Sci*. 2019;21(1):259. doi:10.3390/ijms21010259
24. Ebrahimi T, Rust M, Kaiser SN, et al.  $\alpha$ 1-antitrypsin mitigates NLRP3-inflammasome activation in amyloid  $\beta$ 1-42-stimulated murine astrocytes. *J Neuroinflammation*. 2018;15(1):282. doi:10.1186/s12974-018-1319-x
25. Putteeraj M, Fairuz YM, Teoh SL. MicroRNA dysregulation in Alzheimer's disease. *CNS Neurol Disord Drug Targets*. 2017;16(9):1000–1009. doi:10.2174/1871527316666170807142311
26. Molina-Van den Bosch M, Jacobs-Cachá C, Vergara A, Serón D, Soler MJ. El rol del sistema renina angiotensina a nivel cerebral [The renin-angiotensin system and the brain]. *Hipertens Riesgo Vasc*. 2021;38(3):125–132. Spanish. doi:10.1016/j.hipert.2020.12.001
27. Holmes C. Review: systemic inflammation and Alzheimer's disease. *Neuropathol Appl Neurobiol*. 2013;39(1):51–68. doi:10.1111/j.1365-2990.2012.01307.x
28. Perry VH, Holmes C. Microglial priming in neurodegenerative disease. *Nat Rev Neurol*. 2014;10(4):217–224. doi:10.1038/nrneurol.2014.38
29. Takeda S, Sato N, Morishita R. Systemic inflammation, blood-brain barrier vulnerability and cognitive/non-cognitive symptoms in Alzheimer disease: relevance to pathogenesis and therapy. *Front Aging Neurosci*. 2014;6:171. doi:10.3389/fnagi.2014.00171
30. Schroder K, Zhou R, Tschopp J. The NLRP3 inflammasome: a sensor for metabolic danger? *Science*. 2010;327(5963):296–300. doi:10.1126/science.1184003
31. Zhang Q, Tao X, Xia S, et al. Emodin attenuated severe acute pancreatitis via the P2X ligand-gated ion channel 7/NOD-like receptor protein 3 signaling pathway. *Oncol Rep*. 2019;41(1):270–278. doi:10.3892/or.2018.6844
32. Ha M, Kim VN. Regulation of microRNA biogenesis. *Nat Rev Mol Cell Biol*. 2014;15(8):509–524. doi:10.1038/nrm3838
33. Swarbrick S, Wragg N, Ghosh S, Stolzing A. Systematic review of miRNA as biomarkers in Alzheimer's disease. *Mol Neurobiol*. 2019;56(9):6156–6167. doi:10.1007/s12035-019-1500-y
34. Nagaraj S, Zoltowska KM, Laskowska-Kaszub K, Wojda U. microRNA diagnostic panel for Alzheimer's disease and epigenetic trade-off between neurodegeneration and cancer. *Ageing Res Rev*. 2019;49:125–143. doi:10.1016/j.arr.2018.10.008
35. Millan MJ. Linking deregulation of non-coding RNA to the core pathophysiology of Alzheimer's disease: an integrative review. *Prog Neurobiol*. 2017;156:1–68. doi:10.1016/j.pneurobio.2017.03.004
36. Wang WX, Rajeev BW, Stromberg AJ, et al. The expression of microRNA miR-107 decreases early in Alzheimer's disease. and may accelerate disease progression through regulation of beta-site amyloid precursor protein-cleaving enzyme 1. *J Neurosci*. 2008;28(5):1213–1223. doi:10.1523/JNEUROSCI.5065-07.2008
37. Hébert SS, Horré K, Nicolai L, et al. MicroRNA regulation of Alzheimer's disease amyloid precursor protein expression. *Neurobiol Dis*. 2009;33(3):422–428. doi:10.1016/j.nbd.2008.11.009
38. Absalon S, Kochanek DM, Raghavan V, Krichevsky AM. MiR-26b, upregulated in Alzheimer's disease, activates cell cycle entry, tau-phosphorylation, and apoptosis in postmitotic neurons. *J Neurosci*. 2013;33(37):14645–14659. doi:10.1523/JNEUROSCI.1327-13.2013
39. Müller M, Kuiperij HB, Versleijen AA, et al. Validation of microRNAs in cerebrospinal fluid as biomarkers for different forms of dementia in a multicenter study. *J Alzheimers Dis*. 2016;52(4):1321–1333. doi:10.3233/JAD-160038
40. Du P, Wang J, Han Y, Feng J. Blocking the lncRNA MALAT1/miR-224-5p/NLRP3 axis inhibits the hippocampal inflammatory response in T2DM with OSA. *Front Cell Neurosci*. 2020;14:97. doi:10.3389/fncel.2020.00097